Coherence induced by a train of ultrashort pulses in a Λ-type system

Marco P. Moreno and Sandra S. Vianna*

Departamento de Física, Universidade Federal de Pernambuco, 50670-901 Recife, Pernambuco, Brazil
**Corresponding author: vianna@ufpe.br*

Received January 4, 2011; revised March 10, 2011; accepted March 11, 2011;
posted March 15, 2011 (Doc. ID 140156); published April 15, 2011

We present an analysis of coherent population trapping in a three-level Λ system when excited by an ultrashort pulse train near the one- and two-photon resonances. Numerical results using Bloch equations give the transient response of the system and clearly reveal a comb of electromagnetically induced transparency (EIT) lines. An analytical solution to describe the EIT lines is derived in the steady-state regime and in the weak field limit. Moreover, numerical results indicate that selective velocity spectroscopy makes possible the observation of the comb of EIT lines in Doppler broadening media.

OCIS codes: 270.1670, 270.4180.

1. INTRODUCTION

The optical frequency comb [1] generated by mode-locked femtosecond lasers has played an important role in various fields such as optical frequency metrology [2] and quantum coherent control [3]. Recently, new proposals in the field of quantum information science have emerged [4] such as the implementation of a quantum logic gate controlled through the phase relationship between successive pulses [5]. Most of the applications explore the perfect periodicity of the frequency comb in addition to the fact that one can tune the repetition rate of the mode-locked laser. In particular, when the repetition rate, or its multiples, matches the splitting between the two lower states in a Λ-type system, a coherent population trapping (CPT) [6] is induced. In this context, a very special case is the electromagnetically induced transparency (EIT) [7], i.e., the system is made transparent to a resonant probe field.

EIT in the ultrashort pulse regime was theoretically predicted by Kocharovskaya and Khanin [8]; in fact, they showed that, in the steady-state regime, a train of ultrashort pulses may also induce CPT when interacting with a three-level Λ system. More recently, an analytic iterative treatment was applied to study the transient behavior in a degenerate Λ system [9]. The experimental observation of the EIT signal as a function of the repetition rate of an ultrashort pulse train produced by a mode-locked diode laser was described by Sautenkov *et al.* [10]. Moreover, the repetition rate spectroscopy was explored by Arissian and Diels [11] using a picosecond mode-locked laser.

In this article, we present an analytical solution for the coherence induced by a long train of ultrashort optical pulses in a three-level lambda system, near the conditions of one- and two-photon resonances. The solution is obtained in the frequency domain, and it is valid for the stationary regime and in the weak field limit. Two assumptions are important. One is related to the fact that a mode-locked laser generates an infinite train of very regular ultrashort pulses that, in the frequency domain, gives a comb of narrow lines that can be written as delta functions. The other is related to the atomic system, for which all the atomic relaxation times are considered longer than the laser repetition period. In this case, the atom interacts not only with the spectrum of a single pulse but with the frequency comb of the pulse train; in fact, the effect is similar to that of an atom interacting with an infinite number of cw lasers whose frequency separation is equal to the repetition rate and having zero relative phases. This behavior can be understood using a physical picture, analogous to the Ramsey fringes, where constructive and destructive interferences, due to the time-delayed phases acquired with the succession of the pulses, occur during the atomic relaxation times. This description allows us to make comparisons with EIT results obtained using cw lasers.

Before discussing the stationary regime, we analyze the temporal evolution of the atomic population and coherence as a function of the laser field intensity, and the number of driving pulses in the excitation train. The interaction of each pulse with the atomic system is described by the optical Bloch equations, and the response of the medium, obtained by a direct numerical integration, is compared with our analytical results.

Our treatment for the problem is based on the scheme of Fig. 1(a). We consider a three-level atom in a Λ configuration interacting with a train of ultrashort pulses generated by a mode-locked laser. Following [12] and taking into account the pulse-to-pulse phase shift, $\Delta\phi - \omega_c T_R$, the total electric field for the pulse train can be written as

$$E(t) = \sum_{n=0}^{N-1} \mathcal{E}(t - nT_R) e^{i(\omega_c t - n\omega_c T_R + n\Delta\phi)}, \tag{1}$$

where $\mathcal{E}(t)$ is the envelope function, ω_c is the angular frequency of the carrier, and T_R is the time between pulses.

The Hamiltonian of the system is given by $\hat{H} = \hat{H}_0 + \hat{H}_{\text{int}}$, where $\hat{H}_0 = \hbar\omega_{12}|2\rangle\langle 2| + \hbar\omega_{13}|3\rangle\langle 3|$ is the Hamiltonian of the free atom, with $\omega_{ij} = \omega_j - \omega_i$, and the coupling between the atom and the electric field reads

$$\hat{H}_{\text{int}} = -\mu_{13}E(t)|1\rangle\langle 3| - \mu_{23}E(t)|2\rangle\langle 3| + \text{h.c.} \tag{2}$$

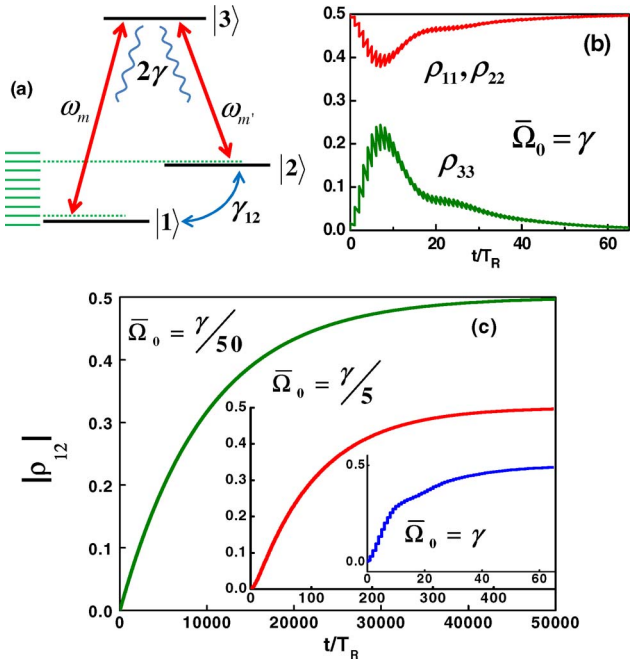

Fig. 1. (Color online) (a) Schematic representation of the three-level Λ system, where ω_m and $\omega_{m'}$ are two distinct modes of the frequency comb. Temporal evolution of the (b) populations $(\rho_{11}, \rho_{22}, \rho_{33})$ and (c) coherence between the two lower states ($|\rho_{12}|$), during the interaction with a train of pulses, obtained by direct numerical integration of Eqs. (3)–(8).

The Bloch equations describing the temporal evolution of the elements ρ_{kl} of the atomic density matrix are given by

$$\dot{\rho}_{33} = [i\Omega_{31}(t)\rho_{13} + \text{c.c.}] + [i\Omega_{32}(t)\rho_{23} + \text{c.c.}] - 2\gamma\rho_{33}, \quad (3)$$

$$\dot{\rho}_{22} = [i\Omega_{23}(t)\rho_{32} + \text{c.c.}] + \gamma\rho_{33}, \quad (4)$$

$$\dot{\rho}_{11} = [i\Omega_{13}(t)\rho_{31} + \text{c.c.}] + \gamma\rho_{33}, \quad (5)$$

$$\dot{\rho}_{23} = (i\omega_{23} - \gamma)\rho_{23} + i\Omega_{23}(t)(\rho_{33} - \rho_{22}) - i\Omega_{13}(t)\rho_{21}, \quad (6)$$

$$\dot{\rho}_{13} = (i\omega_{13} - \gamma)\rho_{13} + i\Omega_{13}(t)(\rho_{33} - \rho_{11}) - i\Omega_{23}(t)\rho_{12}, \quad (7)$$

$$\dot{\rho}_{12} = (i\omega_{12} - \gamma_{12})\rho_{12} - i\Omega_{32}(t)\rho_{13} + i\Omega_{13}(t)\rho_{32}, \quad (8)$$

where γ_{12} is the relaxation rate of the coherence ρ_{12}, and $\Omega_{kl}(t) = \mu_{kl}E(t)/\hbar$ is the time-dependent Rabi frequency for the transition with electric dipole moment μ_{kl}. We consider that the transition $|1\rangle \rightarrow |2\rangle$ between the two lower states is dipole-forbidden and that the spontaneous decay rate of the excited state $|3\rangle$, 2γ, is smaller than the pulse repetition rate, $f_R = 1/T_R$. In this case, the atom could never completely relax between two consecutive pulses, leading to accumulation in both population and coherence [13]. In the frequency domain, this means that the atomic system can distinguish between two neighboring modes of the frequency comb.

Three resonance situations are investigated, and the conditions at which the atomic system reaches a stationary state, for each case, are obtained by numerical integration of the Bloch equations using a standard fourth-order Runge–Kutta method. Optical pumping occurs when a mode of the frequency comb matches only one-photon transition [14]: $\nu_{i3} = mf_R + (\Delta\phi/2\pi)f_R$, for $i = 1$ or 2 and m integer. In this case, no net population is obtained at the excited state, and the coherence between the two lower levels, ρ_{12}, evolves to zero. The Raman resonance is characterized by a pure two-photon transition, and it is achieved whenever the pulse repetition rate or its multiples coincides with the frequency difference between the two lower states [15], $\nu_{12} = qf_R$, with q integer. However, the more interesting situation takes place when both one- and two-photon resonances occur simultaneously, which corresponds to the EIT condition. In this case, the stationary regime of maximum coherence is achieved for a number of driving pulses much smaller than that needed for maximum coherence in Raman resonance.

2. NUMERICAL RESULTS

Temporal evolution of the populations, ρ_{11}, ρ_{22}, and ρ_{33}, during the interaction with a train of pulses, when both one- and two-photon resonances occur simultaneously, is shown in Fig. 1(b). The results are similar to those obtained for a degenerate Λ system using an analytic iterative solution [9]. To simplify the numerical computation, we modeled the pulses as having square envelopes with a time duration of $T_p = 100$ fs, and $\Delta\phi = 0$. We have also considered $\mu_{13} = \mu_{23} = \mu$ and defined an average Rabi frequency,

$$\bar{\Omega}_o = \Omega_o \frac{T_p}{T_R}, \quad (9)$$

where Ω_o is the magnitude of the Rabi frequency for the square pulse. In these resonance conditions the coherence between the two lower states, ρ_{12}, is showed in Fig. 1(c), for three values of $\bar{\Omega}_o$. These results are obtained for $\gamma_{12} = 0$, $\nu_{12} = 70f_R$, $\nu_{13} = 4 \times 10^6 f_R$, and $f_R = (50/2\pi)\gamma$. Whereas for weak fields full coherence is reached only after the interaction with more than 50,000 pulses, for $\bar{\Omega}_o$ of the order of γ, full coherence is obtained before 100 driving pulses, and Rabi oscillations (due to coherent accumulation) are observed in both coherence and population [9].

In the stationary regime, the atomic response to the excitation by a train of femtosecond pulses can be studied as a function of the pulse repetition rate. Figure 2 shows (a) the excited-state population, ρ_{33}, and (b) the coherence, $|\rho_{12}|$, as a function of δf_R, i.e., the variation of f_R around the condition $\nu_{12} = 70f_R$. The results were obtained for the same parameters of Fig. 1, with $(\omega_c/2\pi) = \nu_{13}$, $(\gamma/2\pi) = 2$ MHz, and $\bar{\Omega}_o = 2\gamma$, after the interaction of the atomic system with more than 500 driving pulses. The maximum values of the excited-state population, $(\rho_{33})_M$, are modulated by the Raman resonances of the medium. As shown in Fig. 2(a), an increase of $(\rho_{33})_M$ is always observed as f_R approaches the two-photon resonance. However, exactly at the two-photon resonance, $(\rho_{33})_M$ goes to zero [Fig. 2(c)] and the envelope of the coherence $|\rho_{12}|$ reaches its maximum value [Fig. 2(b)]. The dip in the Raman resonance and the maximum value of the $|\rho_{12}|$ envelope are signatures of the EIT window. The experimental observation of these EIT windows, using ultrashort pulses, was reported in [10,11]. In Figs. 2(d) and 2(e) we have a zoom of the two regions inside the Raman resonance. We can clearly see the peaks in ρ_{33} due to the one-photon resonance condition, $\nu_{i3} = mf_R$. The frequency difference between two successive one-photon resonance peaks is given by f_R/m, while the frequency separation between successive EIT windows is determined by f_R/q. We note that, by changing f_R, m and q must adjust accordingly,

so the frequency separations are not equidistant. Moreover, since m is of the order of 4×10^6 [Figs. 2(d) and 2(e)] and q assume the values 69, 70, and 71 [Figs. 2(a) and 2(b)], we have that $f_R/m \sim \mathcal{O}(\text{Hz})$ and $f_R/q \sim \mathcal{O}(\text{MHz})$. Near $\delta f_R = 0$, i.e., when both one- and two-photon resonances are present, a comb of EIT lines is observed, characterized by very narrow dips in ρ_{33}, as shown in Fig. 2(d).

3. ANALYTICAL APPROACH

The strong dependence on the modes of the frequency comb of the atomic population and coherence, as indicated in Fig. 2, can be better understood if, instead of working in the time domain, we look at the frequency domain [16]. We are interested in the atomic response near the two-photon resonance and after a long time interaction with the pulse train as the system reaches the steady-state regime. In the weak pulse limit, we can neglect the variations in the populations and then write $\rho_{33} = 0$, $\rho_{11} = \rho_{11}^f$, and $\rho_{22} = \rho_{22}^f$, where ρ_{11}^f and ρ_{22}^f are the steady-state population values at the one- and two-photon resonances. These two populations depend on the ratio between the electric dipole momenta, μ_{13} and μ_{23}, and they are independent of the initial conditions [17].

We began our treatment in the frequency domain by taking the Fourier transform (FT) of the pulse train [12]:

$$\tilde{E}(\omega) = \frac{2\pi\tilde{\mathcal{E}}(\omega - \omega_c)}{T_R} \sum_{m=-\infty}^{\infty} \delta(\omega - \omega_m). \tag{10}$$

From Eq. (10) we clearly see that the frequency spectrum consists of a comb of very narrow lines with frequencies $\omega_m = (2\pi m + \Delta\phi) f_R$ and zero relative phase.

Using the above-mentioned values for the populations and taking the FT of each term of Eqs. (6)–(8), we can write the atomic coherence, in the frequency domain, as

$$\tilde{\rho}_{12}(\omega) = \frac{1}{(\omega_{12} - \omega) + i\gamma_{12}} \times [\tilde{\Omega}_{32}(\omega) \otimes \tilde{\rho}_{13}(\omega) - \tilde{\Omega}_{13}(\omega) \otimes \tilde{\rho}_{32}(\omega)], \tag{11}$$

$$\tilde{\rho}_{13}(\omega) = \frac{1}{(\omega_{13} - \omega) + i\gamma} \times [\rho_{11}^f \tilde{\Omega}_{13}(\omega) + \tilde{\Omega}_{23}(\omega) \otimes \tilde{\rho}_{12}(\omega)], \tag{12}$$

$$\tilde{\rho}_{23}(\omega) = \frac{1}{(\omega_{23} - \omega) + i\gamma} \times [\rho_{22}^f \tilde{\Omega}_{23}(\omega) + \tilde{\Omega}_{13}(\omega) \otimes \tilde{\rho}_{21}(\omega)], \tag{13}$$

where

$$\tilde{\rho}_{ij}(\omega) = \int_{-\infty}^{\infty} \rho_{ij}(t) e^{-i\omega t} dt,$$

$$\tilde{\Omega}_{ij}(\omega) = 2\pi\bar{\Omega}_{ij} \sum_m \delta(\omega - \omega_m),$$

and $\tilde{\Omega}_{ij}(\omega) \otimes \tilde{\rho}_{kl}(\omega)$ is the convolution between the two functions. We have also considered that all modes of the comb, near the one- and two-photon transitions, have the same amplitude. This allows us to write an average Rabi frequency for each transition $i \to j$:

$$\bar{\Omega}_{ij} = \frac{\mu_{ij}\,\tilde{\mathcal{E}}(\omega_m - \omega_c)}{\hbar T_R},$$

where the amplitude of each mode $\tilde{\mathcal{E}}(\omega_m - \omega_c)$ is equal to the electric field amplitude of the square pulse times the pulse duration T_p; in fact, we can show, for $\mu_{13} = \mu_{23} = \mu$, that $\bar{\Omega}_{ij} = \bar{\Omega}_0 = \Omega_0 T_p / T_R$.

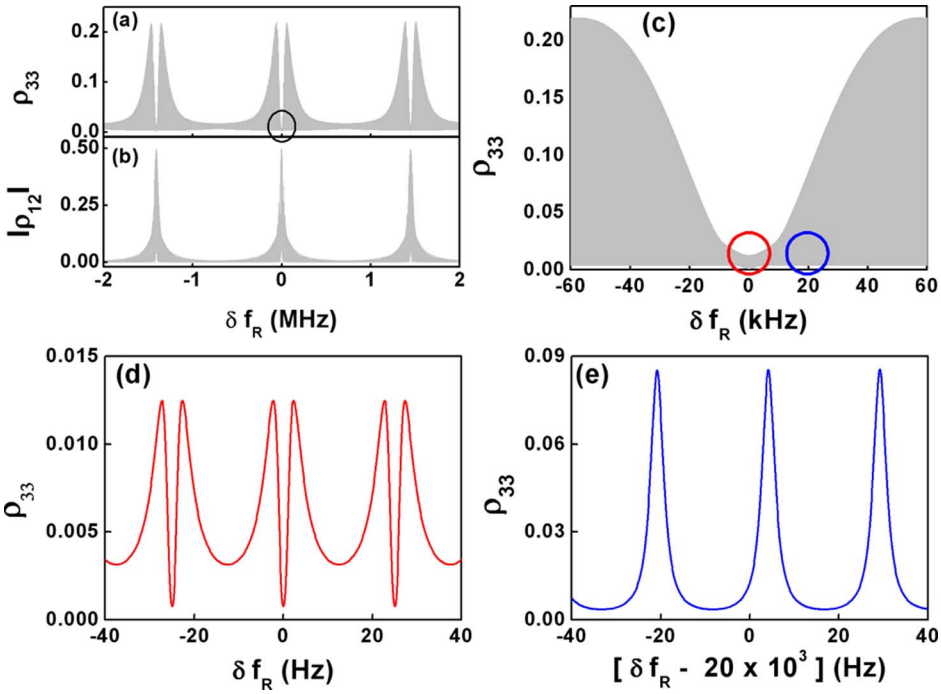

Fig. 2. (Color online) (a) Excited-state population ρ_{33} and (b) coherence $|\rho_{12}|$ as a function of δf_R, for $f_R = 100\,\text{MHz}$, $(\gamma/2\pi) = 2\,\text{MHz}$, $\nu_{12} = q f_R$, with $q = (69, 70, 71)$ and $\bar{\Omega}_o = 2\gamma$, obtained by direct numerical integration of Eqs. (3)–(8). (c) Zoom of the region inside the circle in (a). (d), (e) Zooms of the regions inside the two circles in (c) around $\delta f_R = 0$ and $\delta f_R = 20\,\text{kHz}$, respectively.

Using Eq. (10) and the convolution theorem, we can write

$$\tilde{\Omega}_{ij}(\omega) \otimes \tilde{\rho}_{kl}(\omega) = \bar{\Omega}_{ij} \sum_m \tilde{\rho}_{kl}(\omega - \omega_m). \tag{14}$$

In the weak field limit, we can neglect the processes involving resonances of four or more photons and then obtain an analytical expression for the coherence between the two lower states, which, in the time domain, is written as (see Appendix A)

$$\rho_{12}(t) = \frac{\sum_{m,m'} \frac{\bar{\Omega}_{13}\bar{\Omega}_{32}}{(\omega_{12}-\omega_{m'}+\omega_m)+i\gamma_{12}} \left[\frac{\rho_{11}^f}{(\omega_{13}-\omega_{m'})+i\gamma} - \frac{\rho_{22}^f}{(\omega_{23}+\omega_m)-i\gamma}\right] \exp[i(\omega_{m'}-\omega_m)t]}{1 - \sum_{m,m'} \frac{1}{(\omega_{12}-\omega_{m'}+\omega_m)+i\gamma_{12}} \left[\frac{|\bar{\Omega}_{23}|^2}{(\omega_{13}-\omega_{m'})+i\gamma} - \frac{|\bar{\Omega}_{13}|^2}{(\omega_{23}+\omega_m)-i\gamma}\right]}. \tag{15}$$

The denominator $(\omega_{12} - \omega_{m'} + \omega_m) + i\gamma_{12}$ in Eq. (15) indicates that we select only processes involving two modes of frequency comb. When the frequency difference of these two modes, $\omega_m - \omega_{m'}$, is equal to the splitting between the two lower states, ω_{12}, the atomic system is pumped into a superposition of the two states, and thereby the increase of the coherence ρ_{12} characterizes the EIT condition. In this situation, we also have the contribution of one-photon resonance from each mode, as indicated by the denominators $(\omega_{13} - \omega_{m'}) + i\gamma$ and $(\omega_{23} + \omega_m) - i\gamma$. This can be clearly seen in Fig. 3, where $|\rho_{12}|$ is plotted as a function of the pulse repetition rate. The envelope of the maximum values of the coherence, $|\rho_{12}|_{\max}$, determines the EIT window, and each peak corresponds to a one-photon resonant transition. What we see is the EIT window with a comb of very narrow EIT lines. The results shown in Fig. 3 were obtained for $\rho_{11}^f = \rho_{22}^f = 1/2$, with the two Rabi frequencies equal to $\bar{\Omega}_o = \gamma/50$, and all the other parameters are equal to those of Fig. 1. In these conditions the system reaches a state of full coherence.

We can also use Eq. (15) to obtain the linewidth of the EIT window that modulates the comb of EIT lines. For this, we keep each branch of the Λ transition on resonance and study the variation of $|\rho_{12}|$ over the two-photon resonance (see Appendix B). In the simplest case of equal Rabi frequencies, we find that the EIT window linewidth, $\Delta(\delta f_R)$, can be written as

$$\Delta(\delta f_R) = \frac{\sqrt{3}}{q\pi}\left(\gamma_{12} + \frac{2\bar{\Omega}_o^2}{\gamma}\right), \tag{16}$$

where q is the number of modes between the two lower states. Equation (16) gives the same behavior as obtained in the case of CPT with cw lasers [18]. The first term is due to the relaxation rate of the coherence ρ_{12}, whereas the second term, proportional to the field intensity, describes the power broadening. The factor $\sqrt{3}$ appears because here the modes are scanning over the two legs of the Λ system.

In Figs. 4(a)–4(c) we plot $|\rho_{12}|_{\max}$ as a function of δf_R in order to compare the linewidth of the EIT window obtained from our analytical approach, Eq. (15), with the numerical results calculated from the Bloch equations, Eqs. (3)–(8), for three different values of the average Rabi frequency. For very low field intensity, where the analytical expression is valid, the two curves overlap. For $\bar{\Omega}_o = \gamma/5$ the linewidths

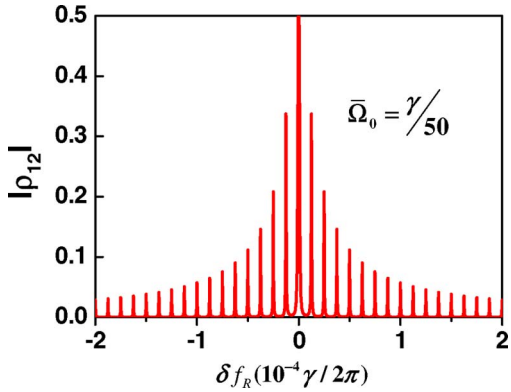

Fig. 3. (Color online) $|\rho_{12}|$ given by Eq. (15) as a function of δf_R.

are almost the same, although differences in the wings of the curve are noted. For $\bar{\Omega}_o = \gamma$ the analytical approach is not longer valid, and thus the numerical results show a narrower window due to saturation effects.

We also remark that the EIT window, as described by $|\rho_{12}|_{\max}$ in Fig. 4, was observed with an ultrashort pulse train produced by a mode-locked diode laser [10] and with a picosecond laser [11]. In the latter experiment, the fluorescence of the excited state was detected, and a decrease of the ρ_{33} population was observed, corresponding to the dip in the Raman resonance as shown in Fig. 2(c).

4. INHOMOGENEOUS BROADENING

As we see in Fig. 3, the excitation of a Λ-type system by a train of ultrashort pulses reveals a series of very narrow EIT lines inside the EIT window. As described before, each narrow EIT line occurs when the system is simultaneously in one- and two-photon resonances [Fig. 2(d)]. However, when we analyze a Doppler broadening atomic sample, for each value of δf_R we need to integrate out the atomic response over the Doppler profile, so the one-photon resonances are blurred and only the dip in the Raman resonance (the EIT window) is observed [19]. To distinguish the one-photon resonances in a Doppler broadening vapor, we can fix the pulse repetition rate and use the velocity selective spectroscopy to probe the atomic response.

In Fig. 5 we show the variation of the lower state population, $\Delta\rho_{11} = \rho_{11} - \rho_{11}^{(o)}$, in the Doppler profile, for a medium

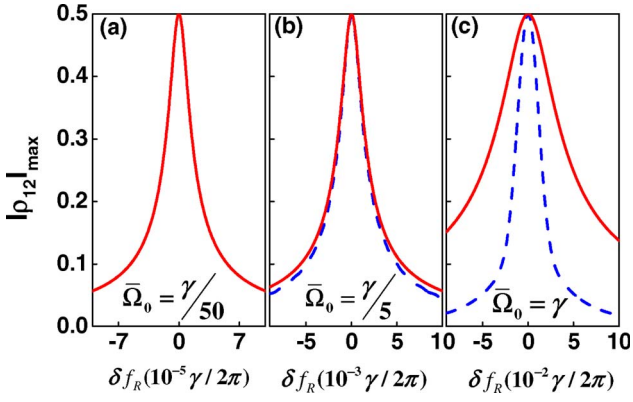

Fig. 4. (Color online) (a)–(c) Comparison between the envelopes of the maximum values of the coherence, $|\rho_{12}|_{\max}$, obtained from Eq. (15) (solid curves) and those obtained by numerical integration of Eqs. (3)–(8) (dashed curves) for three values of $\bar{\Omega}_o$.

with a Doppler width equal to $\omega_D = 250\gamma$ and initial conditions $\rho_{11}^{(o)} = \rho_{22}^{(o)} = 1/2$. The numerical results were obtained from Eqs. (3)–(8), using an average Rabi frequency equal to $\bar{\Omega}_o = \gamma/5$, for both transitions and after the interaction of the atomic system with 1000 driving pulses. To account for the velocity distribution, we replace the transition frequencies ω_{13} and ω_{23} in Eqs. (6)–(8) by $\omega_{13} - \delta$ and $\omega_{23} - \delta$, where $\delta = \vec{k} \cdot \vec{v}$ labels the different atomic velocity groups, and $\vec{k}$ and $\vec{v}$ are the laser wave vector and the atomic velocity, respectively. The other parameters are equal to those of Fig. 2. In Fig. 5(a), $f_R = 100$ MHz, corresponding to the situation where all the atoms are at the two-photon resonance ($\nu_{12} = 70 f_R$), but only groups of atoms with specific velocities will also be at the one-photon resonance and thereby manifest the EIT effect. It is interesting to note that the result shown in Fig. 5(a) also reflects the fact that in the copropagating geometry the two-photon transition is Doppler-free, which is not the case for the one-photon transition.

Last, when we change the pulse repetition rate for a value distinct from a harmonic of ν_{12}, as shown in Fig. 5(b), we observe only the peaks corresponding to the population transfer processes due to the one-photon resonances in each leg of the lambda system for different groups of atoms. The situation described in Fig. 5(b) has been investigated in detail, as a function of the atomic density and laser intensities for the lines D1 and D2 of Rb alkaline metal [20,21]. Moreover, the results shown in Fig. 5(a) indicate that the selective velocity spectroscopy can be used to observe the comb of the EIT lines in the Doppler profile of an inhomogeneously broadened medium.

For a realistic atomic system, we need to consider the hyperfine excited states. In this case, using a laser at the standard 100 MHz repetition rate, which is more feasible to perform our numerical approach, the EIT lines shown in Fig. 5(a) may be blurred. However, the EIT lines for each hyperfine level can be separated if a laser with higher repetition rate, such as 1 GHz, is used [22].

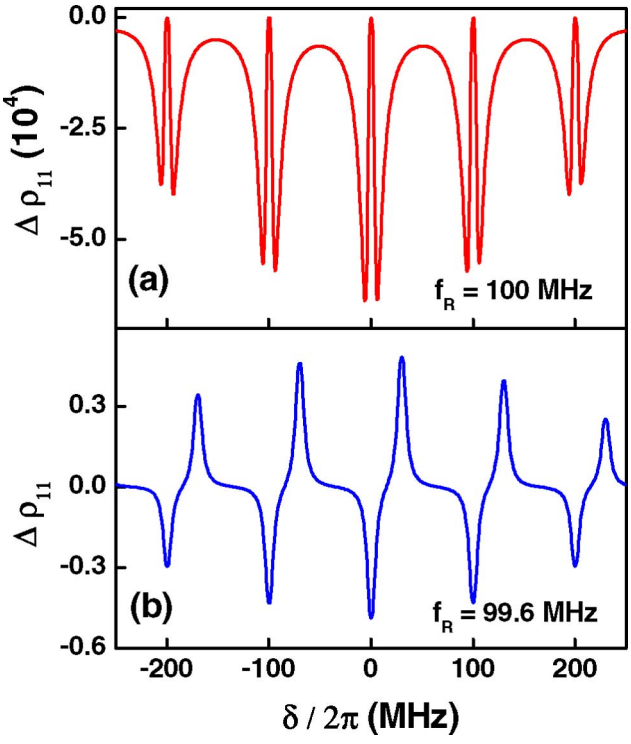

Fig. 5. (Color online) Variation of the lower state population, $\Delta\rho_{11}$, as a function of the atomic velocity groups ($\delta/2\pi$), for a medium with Doppler width equal to $\omega_D = 250\gamma$, $\bar{\Omega}_o = \gamma/5$, and (a) $\nu_{12} = 70 f_R$ (two-photon resonance) and (b) $\nu_{12} = 70.3 f_R$.

5. CONCLUSIONS

In this paper we have presented a study of the CPT in a three-level Λ system excited by an ultrashort pulse train near the one- and two-photon resonances. The temporal evolution of the atomic system and the response to a repetition rate spectroscopy were obtained from the numerical integration of the Bloch equations. The results showed the occurrence of a comb of very narrow EIT lines, determined by the one-photon resonances, that appears inside the EIT windows. While the frequency difference between two successive EIT lines is given by f_R/m, where m is determined by $\nu_{i3} = m f_R$, the frequency separation between successive EIT windows is determined by f_R/q, where q is related to the number of modes between the two lower states. We also worked in the frequency domain to explore a more intuitive physical picture. In this context, we derived a closed analytical solution to describe these EIT signals, which is valid in the weak field regime. In particular, we showed that the linewidth of the EIT window can be modeled by two cw lasers with equal intensities. Further, a comparison of the analytical results with those obtained by a direct numerical integration of the Bloch equations was also present. Finally, the numerical results indicate that selective velocity spectroscopy appears as very useful tool to observe the comb of EIT lines in Doppler broadening media.

APPENDIX A: DERIVATION OF EQ. (15)

Using Eq. (14) to write the convolutions $\tilde{\Omega}_{ij}(\omega) \otimes \tilde{\rho}_{kl}(\omega)$ in Eqs. (11)–(13), we obtain

$$\tilde{\rho}_{12}(\omega) = \frac{1}{(\omega_{12} - \omega) + i\gamma_{12}} \times \left[\sum_m \bar{\Omega}_{32}\tilde{\rho}_{13}(\omega + \omega_m) - \sum_m \bar{\Omega}_{13}\tilde{\rho}_{32}(\omega - \omega_m)\right], \quad \text{(A1)}$$

$$\tilde{\rho}_{13}(\omega) = \frac{1}{(\omega_{13} - \omega) + i\gamma} \times \left[2\pi\rho_{11}^f \bar{\Omega}_{13}\sum_{m'}\delta(\omega - \omega_{m'}) + \sum_{m'}\bar{\Omega}_{23}\tilde{\rho}_{12}(\omega - \omega_{m'})\right], \quad \text{(A2)}$$

$$\tilde{\rho}_{23}(\omega) = \frac{1}{(\omega_{23} - \omega) + i\gamma} \times \left[2\pi\rho_{22}^f \bar{\Omega}_{23}\sum_{m'}\delta(\omega - \omega_{m'}) + \sum_{m'}\bar{\Omega}_{13}\tilde{\rho}_{21}(\omega - \omega_{m'})\right]. \quad \text{(A3)}$$

As we are interested in the coherence between the two lower states, we use Eqs. (A2) and (A3) to obtain $\tilde{\rho}_{13}(\omega + \omega_m)$ and $\tilde{\rho}_{32}(\omega - \omega_m)$ and thus insert them into Eq. (A1). We find

$$\tilde{\rho}_{12}(\omega) = \frac{1}{(\omega_{12}-\omega)+i\gamma_{12}} \times \sum_{m,m'}\left\{2\pi\bar{\Omega}_{13}\bar{\Omega}_{23}\left[\frac{\rho_{11}^{f}}{(\omega_{13}-\omega-\omega_m)+i\gamma} - \frac{\rho_{22}^{f}}{(\omega_{23}-\omega+\omega_{m'})-i\gamma}\right]\delta(\omega+\omega_m-\omega_{m'}) + \left[\frac{|\bar{\Omega}_{23}|^2}{(\omega_{13}-\omega-\omega_m)+i\gamma} - \frac{|\bar{\Omega}_{13}|^2}{(\omega_{23}-\omega+\omega_{m'})-i\gamma}\right] \times \tilde{\rho}_{12}(\omega+\omega_m-\omega_{m'})\right\}. \quad \text{(A4)}$$

Equation (A4) allows an iterative solution for $\tilde{\rho}_{12}(\omega)$. A closed solution is obtained in the weak field limit, when only two-photon resonances are considered. In this case, we can take $\tilde{\rho}_{12}(\omega+\omega_m-\omega_{m'}) \approx \tilde{\rho}_{12}(\omega)$ and thus obtain

$$\tilde{\rho}_{12}(\omega) = \frac{\frac{2\pi\bar{\Omega}_{13}\bar{\Omega}_{32}}{(\omega_{12}-\omega)+i\gamma_{12}}\sum_{m,m'}\left[\frac{\rho_{11}^{f}}{(\omega_{13}-\omega-\omega_m)+i\gamma} - \frac{\rho_{22}^{f}}{(\omega_{23}-\omega+\omega_{m'})-i\gamma}\right]\delta(\omega+\omega_m-\omega_{m'})}{1-\frac{1}{(\omega_{12}-\omega)+i\gamma_{12}}\sum_{m,m'}\left[\frac{|\bar{\Omega}_{23}|^2}{(\omega_{13}-\omega-\omega_m)+i\gamma} - \frac{|\bar{\Omega}_{13}|^2}{(\omega_{23}-\omega+\omega_{m'})-i\gamma}\right]}. \quad \text{(A5)}$$

So the coherence between the two lower states, in the stationary regime, is given by the FT of Eq. (A5) and is displayed in Eq. (15).

APPENDIX B: DERIVATION OF EQ. (16)

In order to derive the linewidth of the EIT window, we consider only the two modes (m and m') of the comb frequency that are near the Raman resonance. In this case, we can set $\delta f_R = \nu_{12}/(m-m')$. By assuming one-photon resonances $\omega_{13} = \omega_{m'}$ and $\omega_{23} = \omega_m$, we can write Eq. (15) as

$$\rho_{12}(t) = \frac{1}{2}\left\{\frac{-\exp(i\omega_{12}t)}{1-\frac{(i\gamma)[i\gamma_{12}-2\pi(m'-m)\delta f_R]}{2|\bar{\Omega}_o|^2}}\right\}, \quad \text{(B1)}$$

where, to simplify, we took $\bar{\Omega}_{13} = \bar{\Omega}_{23} = \bar{\Omega}_o$ and $\rho_{11}^{f} = \rho_{22}^{f} = 1/2$.

The maximum value for the coherence ρ_{12} is achieved at the two-photon resonance, i.e., $\delta f_R = 0$:

$$|\rho_{12}|_{(\delta f_R=0)} = \frac{1}{2}\left(\frac{1}{1+\frac{\gamma\gamma_{12}}{2|\bar{\Omega}_o|^2}}\right). \quad \text{(B2)}$$

The linewidth $\Delta(\delta f_R)$ is determined by the values of δf_R at $|\rho_{12}| = \frac{1}{2}|\rho_{12}|_{(\delta f_R=0)}$ and is given by Eq. (16).

ACKNOWLEDGMENTS

We acknowledge helpful discussions with D. Felinto and L. H. Acioli. This work was supported by the Brazilian agencies Conselho Nacional de Desenvolvimento Científico e Tecnológico, Fundação de Amparo à Ciência e Tecnologia do Estado de Pernambuco, and Coordenação de Aperfeiçoamento de Pessoal de Nível Superior.

REFERENCES AND NOTES

1. T. Udem, R. Holzwarth, and T. W. Hänsch, "Optical frequency metrology," Nature **416**, 233–236 (2002).
2. J. Ye and S. T. Cundiff, *Femtosecond Optical Frequency Comb Technology: Principle, Operation, and Applications* (Springer, 2005).
3. M. C. Stowe, A. Pe'er, and J. Ye, "Control of four-level quantum coherence via discrete spectral shaping of an optical frequency comb," Phys. Rev. Lett. **100**, 203001 (2008).
4. G. Campbell, A. Ordog, and A. I. Lvovsky, "Multimode electromagnetically induced transparency on a single atomic line," New J. Phys. **11**, 103021 (2009).
5. D. Hayes, D. N. Matsukevich, P. Maunz, D. Hucul, Q. Quraishi, S. Olmschenk, W. Campbell, J. Mizrahi, C. Senko, and C. Monroe, "Entanglement of atomic qubits using an optical frequency comb," Phys. Rev. Lett. **104**, 140501 (2010).
6. E. Arimondo, "Coherent population trapping in laser spectroscopy," Prog. Opt. **35**, 257–355 (1996).
7. M. Fleischhauer, A. Imamoglu, and J. P. Marangos, "Electromagnetically induced transparency: optics in coherent media," Rev. Mod. Phys. **77**, 633–673 (2005).
8. O. A. Kocharovskaya and Y. I. Khanin, "Population trapping and coherence bleaching of a three-level medium by a periodic train of ultrashort pulses," Sov. Phys. JETP **63**, 945–950 (1986).
9. A. A. Soares and L. E. E. de Araujo, "Coherent accumulation of excitation in the electromagnetically induced transparency of an ultrashort pulse train," Phys. Rev. A **76**, 043818 (2007).
10. V. A. Sautenkov, Y. V. Rostovtsev, C. Y. Ye, G. R. Welch, O. Kocharovskaya, and M. O. Scully, "Electromagnetically induced transparency in rubidium vapor prepared by a comb of short optical pulses," Phys. Rev. A **71**, 063804 (2005).
11. L. Arissian and J.-C. Diels, "Repetition rate spectroscopy of the dark line resonance in rubidium," Opt. Commun. **264**, 169–173 (2006).
12. S. T. Cundiff, "Phase stabilization of ultrashort optical pulses," J. Phys. D **35**, R43–R59 (2002).
13. D. Felinto, C. A. C. Bosco, L. H. Acioli, and S. S. Vianna, "Coherent accumulation in two-level atoms excited by a train of ultrashort pulses," Opt. Commun. **215**, 69–73 (2003).
14. D. Aumiler, T. Ban, H. Skenderović, and G. Pichler, "Velocity selective optical pumping of Rb hyperfine lines induced by a train of femtosecond pulses," Phys. Rev. Lett. **95**, 233001 (2005).
15. J. Mlynek, W. Lange, H. Harde, and H. Burggraf, "High-resolution coherence spectroscopy using pulse trains," Phys. Rev. A **24**, 1099–1102 (1981).
16. T. H. Yoon, A. Marian, J. L. Hall, and J. Ye, "Phase-coherent multilevel two-photon transitions in cold Rb atoms: ultrahigh-resolution spectroscopy via frequency-stabilized femtosecond laser," Phys. Rev. A **63**, 011402(R) (2000).
17. R. M. Whitley and C. R. Stroud, Jr., "Double optical resonance," Phys. Rev. A **14**, 1498–1513 (1976).
18. J. Vanier, A. Godone, and F. Levi, "Coherent population trapping in cesium: dark lines and coherent microwave emission," Phys. Rev. A **58**, 2345–2358 (1998).
19. D. Aumiler, "Coherent population trapping in ^{87}Rb atoms induced by the optical frequency comb excitation," Phys. Rev. A **82**, 055402 (2010).
20. T. Ban, D. Aumiler, H. Skenderovic, S. Vdovic, N. Vujiic, and G. Pichler, "Cancellation of the coherent accumulation in rubidium atoms excited by a train of femtosecond pulses," Phys. Rev. A **76**, 043410 (2007).
21. M. Polo, C. A. C. Bosco, L. H. Acioli, D. Felinto, and S. S. Vianna, "Coupling between cw lasers and a frequency comb in dense atomic samples," J. Phys. B **43**, 055001 (2010).
22. Our preliminary results, using a femtosecond laser with 1 GHz repetition rate, show that the two hyperfine excited states of the D1 line of Rb 85 are well resolved in the Doppler profile (unpublished).